Mapping Strain in Nanocrystalline Nitinol: an X-ray Diffraction Method

Matthew Bibee

Office of Science, SULI Program

University of California, San Diego

Stanford Linear Accelerator Center

Menlo Park, California

August 19, 2005

Prepared in partial fulfillment of the requirements of the Office of Science, U.S. Department of Energy Science Undergraduate Laboratory Internship (SULI) Program under the direction of Dr. Apurva Mehta in the of the Stanford Synchrotron Radiation Laboratory (SSRL) at the Stanford Linear Accelerator Center (SLAC).

Participant: _____
Signature

Research Advisor: _____
Signature

Work supported by Department of Energy contract DE-AC02-76SF00515

Table of Contents

ABSTRACT

Mapping Strain in Nanocrystalline Nitinol: an X-ray Diffraction Method. MATTHEW BIBEE (University of California, San Diego, La Jolla, CA 92093) APURVA MEHTA (Stanford Linear Accelerator Center, Menlo Park, CA 94025).

Understanding the mechanical properties of biomedical devices is critical in predicting and preventing their failure in the body. Such knowledge is essential, for example, in the design of biomedical stents, which must undergo repeated strain over their ten year lifetimes without breaking. Computational models are used to predict mechanical response of a device, but these models are not complete; there are significant deviations from the predictions, especially when devices are subjected to repeated multi-axial loads. Improving these models requires comparisons with actual measurements of strained nitinol. Local measurements of the full strain tensor can be made using X-ray diffraction techniques, but they are currently limited to materials whose grain size is larger than the X-ray beam size or require several diffraction patterns produced by rotation of the sample. Nitinol stents are nanocrystalline, with grains smaller than any available X-ray beam. We present a method for measuring the local strain in a nanocrystalline material from a single X-ray diffraction pattern by extending current powder diffraction techniques. The components of the strain tensor are mapped onto a displacement ellipsoid, which is then reconstructed from diffraction data through Bragg's law and least-squares fitting. Using simulated diffraction data, we performed sensitivity tests to examine how the accuracy of the method depends on how much of the diffraction pattern is measured. We found that strain can be accurately calculated from measurements of at least three

diffraction arcs of at least 20° in length. Thus we believe that our method is a viable approach to calculating strain provided a sufficient amount of diffraction pattern is recorded.

INTRODUCTION

Designing biomedical devices requires a detailed understanding of the materials from which they are constructed in order to minimize the risk of failure inside the body. One vital property that affects a device's durability is the material's stress-strain behavior. For instance, a biomedical stent (a metal mesh tube used to prop open a collapsed artery) must expand and contract each time the heart beats. Thus, over a stent's FDA-required lifetime of ten years, it must undergo more than four-hundred million strain cycles without breaking. Thus knowledge of how strain affects the integrity of a material is critical for stent design.

Designing a device to withstand such large amounts of repeated strain is complicated, but powerful computational finite element models exist to predict the strain behavior of nitinol in biomedical stents [1] These models aid greatly in stent design, but the fact that stent failures still occur shows that the models are not complete. Incompleteness of the FEA models also arises from the fact that more and more biomedical devices are made from advanced materials, such as nitinol. Nitinol, an equiatomic alloy of nickel and titanium, is used in stent production because of its unique properties of superelasticity and shape memory. While these properties are an asset in the creation of stents, they also cause nitinol's strain behavior to differ markedly from that of more well-studied materials such as steel. In addition to the reversible elastic and nonreversible plastic deformation documented in steel, nitinol can also deform by a reversible, temperature dependent transformation between austenite and martensite phases. It is this extra mechanism of deformation that provides nitinol with its unusual superelastic and shape

memory properties and also contributes to less than adequate understanding of its mechanical response under repeated multi-axial load.

In order to improve the models it is necessary to directly measure strain in a real device. X-ray diffraction, being non-contact and non-destructive, is a useful method for measuring local strain on a device which is still under a complex multi-axial load. However, its usefulness is currently limited by the size of the X-ray beam (currently about 1 m at U.C. Berkeley's Advanced Light Source). Successful strain measurements have been made for materials whose grains are larger than the beam size [2]. In this arrangement, the beam is incident on a single crystallite, creating a Laue diffraction pattern that can be used to calculate the second rank (three-by-three) strain tensor. However, when the grains are smaller than the beam size, the beam is diffracted by many crystallites at once. This is the case for nanocrystalline nitinol, which is the primary material for stent production. Strain has not yet been measured in these materials, but we propose that it is possible to calculate the local strain tensor of nanocrystalline nitinol using powder diffraction techniques similar to those described by [3] and [4]. However, in contrast to their techniques, we calculate the strain tensor from a single diffraction pattern rather than a series of patterns recorded at different sample orientations. Measuring local strain at many locations in a sample produces a strain map of the material's response to a given stress condition. Comparison of strain maps from measurement and modeling helps to improve the models, resulting in the creation of more reliable stents.

MATERIALS AND METHODS

Effects of Strain on a Material

While bulk strain is easily measurable using a strain gauge, local strain measurements are considerably more difficult. The imposition of stress on a material produces changes in the material's macroscopic dimensions, which manifest themselves on the atomic level as alterations to the crystal lattice. A material under elastic strain will deform due to the compression and stretching of atomic bonds, which alters the spacing of the crystal lattice planes. Strain is represented mathematically by a symmetric second order tensor consisting of six independent terms: three terms representing normal strain and three representing shear strain. However, the strain tensor may always be transformed by coordinate system rotation into a system where shear strains vanish and the normal strains are defined as the principal strains. With no shear strain, it is evident that a tensile normal strain represents an increase in atomic spacing along the axis of the strain, whereas a compressive normal strain represents a corresponding decrease in atomic spacing. Thus we can conceive of a displacement ellipsoid, oriented along the three principal strain axes, whose deviations from a sphere correspond to the principle strains. The ellipsoid will be thinner than the unstrained sphere along axes of compressive strain and thicker along axes of tensile strain. The addition of shear strain produces a rotation of the ellipsoid.

X-ray Diffraction

X-ray diffraction is an excellent tool for examining the spacing between atoms and, by extension, strain. When an X-ray beam is incident upon a single crystal, the radiation that is

scattered from each atom will interfere constructively only at certain angles relative to the crystal lattice, creating a series of diffraction spots. For a comprehensive explanation of scattering and diffraction, see [5]. The angles at which the spots will appear are given by Bragg's law,

$$\frac{2d\sin\theta}{\lambda} = n,$$

where is the X-ray wavelength, d is the spacing of the diffraction planes, is the angle of beam incidence and diffraction, and n is an integer. d is measured along the bisector of the incident and diffracted beams. Following conventions of diffraction notation, we will refer henceforth to the angle 2 rather than . The spacing of the diffraction spots, measured by 2 , is thus inversely proportional to the crystal lattice spacing d.

Nanocrystalline nitinol by definition is made of grains on the order of several nanometers, much smaller than the beam size of 1 m. Thus the X-ray beam is incident upon many small crystallites at once. We assume that the crystal lattices of the crystallites are oriented randomly with respect to one another. In this situation, often called powder diffraction, each grain illuminated by the beam produces its own set of diffraction spots with the same angle 2 from single crystal diffraction. Assuming the crystallites are randomly oriented with respect to one another, each diffraction spot smears out into a ring (Figure 2), with each point on a ring corresponding to the diffraction spot produced by the crystallites sharing a certain orientation. The orientation of the crystallite is represented by the angle , which is the angle that the crystallite's diffraction spot has been rotated away from vertical. Several distinct rings will be present in the pattern, corresponding to d spacings of the different sets of diffraction planes defined by the crystal's specific Bravais lattice type [5]. Typically

only part of each ring is captured by a detector, so that a powder diffraction pattern appears as a set of “ -arcs,” each of which represents a constant 2 value and a range of values (Figure 1).

Calculation of the Strain Tensor

Techniques exist for calculating local strain in materials using single crystal diffraction [2] and from powder diffraction patterns using multiple beam shots at a number of different incident angles [3,4]. Our method extends the work of [3] and [4] to allow the local strain tensor to be calculated from a single diffraction pattern, which not only eliminates the technical challenge of focusing the X-ray beam on a single area of sample while changing the angle of incidence, but it also reduces the time required to complete a measurement.

The key to our technique is the fact that crystallites with different orientations will have different responses to an applied strain. The magnitude and sign of the change in spacing between the lattice planes is dependent on the relative orientation of the lattice planes and the local principal strain axes. The change in diffraction plane spacing along a given axis is directly equivalent to the deviation of the displacement ellipse from the unstrained sphere along that axis. Importantly, the lattice spacing d now varies with angles 2 and , meaning the -arcs no longer represent constant 2 values. Each point on each arc provides information about the local strain along a particular axis specified by 2 and . The strain can be calculated from

$$\varepsilon_{2\theta,\chi} = \frac{d_{2\theta,\chi} - d_0}{d_0},$$

where $d_{2,}$ is the lattice spacing measured along this axis and d_0 is the unstrained lattice spacing, which can be measured from an unstrained sample. $d_{2,}$ and d_0 can be calculated using Bragg's law.

A single -arc provides d values over a range of 's, and several -arcs together provide d values over a range of 's at several 2 values. Each -arc is produced by a different set of diffraction planes, meaning each arc has a different d value, however the d values are not independent and can be normalized using a single multiplicative factor derived from the crystal lattice structure (for nitinol, these factors are $1, \sqrt{2}, \sqrt{3}, 2, \ldots$). When normalized, the diffraction arcs can be transformed into arcs that can thought of as lying on a single displacement ellipsoid (Figure 3).

[3] and [4] describe how to calculate the six terms of the strain tensor given a set of normalized d values measured at different angles. However, the coordinate system used by [3] and [4] is designed to accommodate measurements made by rotating the sample or X-ray beam, not measurements extracted from the -arcs. Therefore, we derived a transformation between the coordinate system of [3] and [4] (shown in Figure 3) and a coordinate system more appropriate for describing -arcs (Figure 4). Modifying equation 5.4 from [4] to use the angles and , where $\omega = \Theta - \frac{2\theta}{2}$ (being the incident angle of the X-ray beam), we get:

$$\varepsilon_{\omega,\chi} = \varepsilon_{11}\frac{\tan^2\omega}{\tan^2\omega+\sec^2\chi} + \varepsilon_{22}\frac{\tan^2\chi}{\tan^2\omega+\sec^2\chi} + \varepsilon_{33}\frac{1}{\tan^2\omega+\sec^2\chi}$$
$$+ \varepsilon_{12}\frac{2\tan\omega\tan\chi}{\tan^2\omega+\sec^2\chi} + \varepsilon_{23}\frac{2\tan\chi}{\tan^2\omega+\sec^2\chi} + \varepsilon_{13}\frac{2\tan\omega}{\tan^2\omega+\sec^2\chi}$$

where $_{11}$, $_{22}$, $_{33}$, $_{12}$, $_{23}$, and $_{13}$ are the six terms of the strain tensor. Each point on each arc yields values for , , and . The non-linear equation in two terms can be transformed into a linear equation in 6 terms,

$$\varepsilon_{\omega\chi} = \varepsilon_{11}a_1 + \varepsilon_{22}a_2 + \varepsilon_{33}a_3 + \varepsilon_{12}a_4 + \varepsilon_{23}a_5 + \varepsilon_{13}a_6$$

where a_1 to a_6 are defined as follows:

$$a_1 = \frac{\tan^2\omega}{\tan^2\omega + \sec^2\chi}$$

$$a_2 = \frac{\tan^2\chi}{\tan^2\omega + \sec^2\chi}$$

$$a_3 = \frac{1}{\tan^2\omega + \sec^2\chi}$$

$$a_4 = \frac{2\tan\omega\tan\chi}{\tan^2\omega + \sec^2\chi}$$

$$a_5 = \frac{2\tan\chi}{\tan^2\omega + \sec^2\chi}$$

$$a_6 = \frac{2\tan\omega}{\tan^2\omega + \sec^2\chi}$$

The terms of the strain tensor can be found by a least squares fit of the diffraction data to the equation above.

A strain map can be obtained by measuring the local strain tensor at a series of grid points along the sample. The map is then created by plotting the values of each component of the tensor spatially.

RESULTS

In order to determine how much data is required for an accurate and robust determination of the strain tensor, we performed several sensitivity tests using simulated diffraction data. We created simulated data of various sizes in order to test the method's

dependence on space coverage. The data was simulated from a tensor with normal strains along the X, Y, and Z axes but no shear strains. Various amounts of Gaussian error were added to the data. Even with perfect data points (no simulated error), tests showed that data from one or two -arcs was insufficient for calculating the full strain tensor. With two arcs, it was possible to calculate the terms $_{22}$, $_{12}$, and $_{23}$ but not $_{11}$, $_{33}$, and $_{13}$. With error-free data and at least three arcs, it was possible to calculate all six terms as long as at least nine data points were available. The results in Figure 5a-f were obtained from simulated data that included points from 3 -arcs with Gaussian errors (standard deviation of 0.1°) added to the values of the simulated data set. The vertical axis shows the deviation of the calculated strain values from the true strain values, and the X axis shows the length of the arcs in degrees of . It was possible to calculate the full strain tensor from the three arcs, but as can be seen in Figure 5b, the accuracy of $_{22}$ declined dramatically for ranges of less than 20°.

DISCUSSION AND CONCLUSION

Our tests show that this method is applicable to nanocrystalline materials if sufficient diffraction data is available. There must be at least three measurable diffraction arcs in the pattern, and the arcs must have sufficient extent. It is evident from the sensitivity tests that the number of arcs sets the goodness of the fit in the XZ plane (where $_{11}$ and $_{33}$ were located), and the length of the arcs sets the goodness of the fit in the Y direction (where $_{22}$ was located). The question is essentially how much of the displacement ellipsoid needs to be measured, and at what accuracy, in order to correctly extrapolate the rest of the ellipsoid. Our results show that at least three -arcs 20° in length are necessary.

The method is also limited by several assumptions. The first assumption is that strain in the material is continuous, so that neighboring crystallites experience the same local strain. If this were not so, then there would be no correlation between different points on the diffraction pattern, and no strain information could be extracted. The grain-to-grain strain discontinuity would results in discreet "jumps" in the diffraction ring. The fact that these jumps are not observed in the diffraction pattern shows that this assumption is mostly true, however, the jumps could still exist on a small scale, manifesting themselves as error in ring measurements. Another assumption is the random orientation of crystallites. In fact, most materials have preferred crystallite orientations due to rolling and other metallurgical shaping processes. Such texture properties lead to imperfections in the diffraction pattern, such as the irregularities in intensity across the diffraction arcs evident in Figure 1. Gaps in the diffraction arcs may be present if there are crystallite orientations which are not sufficiently populated in the material. Such gaps reduce the space available for measurement and thus affect the accuracy of the fit. An additional assumption is the absence of plastic strain. This method measures only elastic strain, as this is the mechanism that affects lattice spacing. A real device under complex multi-axial load undergoes both plastic and elastic deformations, so it is important to minimize the amount of plastic strain by simplifying the load geometry and limiting the total strain on the material. The austenite-martensite transition also occurs as strain increases, so that in some cases the cubic austenite arcs may be replaced with monoclinic martensite arcs. One must be vigilant for this transition, but new arcs are easily discernable and can be incorporated into the method, yielding a measure of the strain associated with the phase transition.

There is still a need to examine the influence of the detector resolution on the goodness of the fit. Once the errors are well understood, the next step is to measure real local strain values and compare the resulting strain maps to the predictions of FEA models such as those in [1]. This will allow refinement of the models, which will provide insight into the physical mechanisms behind nitinol deformation. Understanding these mechanisms is vital to producing safer and longer lasting stents.

ACKNOWLEDGEMENTS

I would like to thank Apurva Mehta, a great mentor in every sense of the word, both scientifically and personally. Xiao-Yan Gong, Alan Pelton, and others at Nitinol Devices and Components were very supportive and provided motivation and background for this research. I would also like to thank the U.S. Department of Energy for providing this research experience, as well as James Lindesay and Helen Quinn for organizing it.

REFERENCES

[1] A. R. Pelton, X. Y. Gong, and T. Duerig, "Fatigue testing of diamond-shaped specimens," *Proceedings of the International Conference on Shape Memory and Superelastic Technology Conference*, 2003.

[2] A. A. MacDowell, R. S. Celestre, N. Tamura, R. Spolenak, B. C. Valek, W. L. Brown, J. C. Bravman, H. A. Padmore, B. W. Batterman, J. R. Patel, "Submicron X-ray diffraction," *Nuclear Instruments and Methods in Physics Research A*, vol. 467-468, 2001, p. 936-943.

[3] V. Hauk, *Structural and residual stress analysis by nondestructive methods*, 1997, pp. 132-133.

[4] I. C. Noyan and J. B. Cohen, *Residual Stress: measurement by diffraction and interpretation*, 1987, pp. 117-130.

[5] B.E. Warren, *X-ray diffraction*, 1990.

Figures

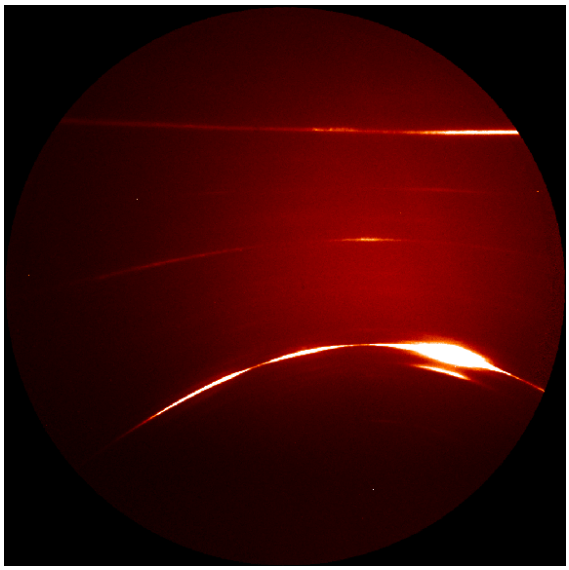

Figure 1. Example of nanocrystalline X-ray diffraction pattern with -arcs.

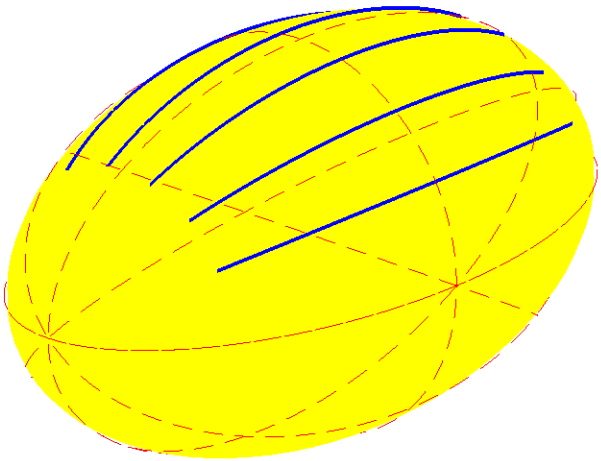

Figure 2. Displacement ellipsoid with -arcs.

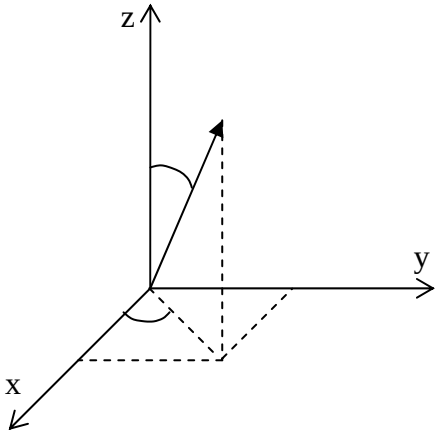

Figure 3. Coordinate system used by [4] and [5].

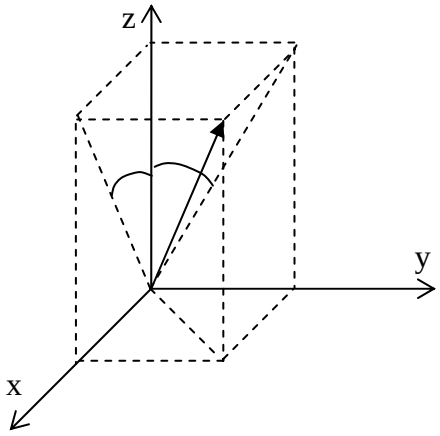

Figure 4. Coordinate system for describing -arcs.

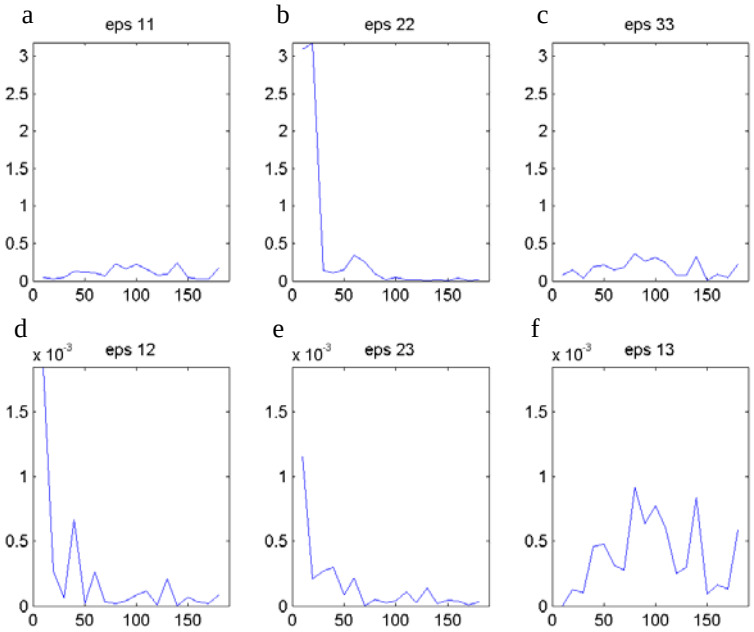

Figure 5. Error in strain term vs. coverage